The autocrine CXCR4/CXCL12 axis contributes to lung fibrosis through modulation of lung fibroblast activity

FEI LI[1], XUEFENG XU[1], JING GENG[2], XUAN WAN[3] and HUAPING DAI[2]

[1]Department of Pulmonary and Critical Care Medicine, Beijing An-Zhen Hospital, Capital Medical University; [2]Department of Pulmonary and Critical Care Medicine, Center of Respiratory Medicine, China-Japan Friendship Hospital, Capital Medical University, National Clinical Research Center for Respiratory Diseases, Beijing 100029; [3]Department of Pulmonary and Critical Care Medicine, First Affiliated Hospital of Nanchang University, Nanchang, Jiangxi 330006, P.R. China

Received December 25, 2018; Accepted October 30, 2019

DOI: 10.3892/etm.2020.8433

Abstract. The C-X-C Motif Chemokine Receptor 4/C-X-C Motif Chemokine Ligand 12 (CXCR4/CXCL12) axis has been implicated in the pathogenesis of pulmonary fibrosis. However, the mechanisms governing this remain to be determined. The current study demonstrated that human lung fibroblasts (HLFs) exhibit high CXCL12 expression and also exhibit high expression of its corresponding receptor CXCR4. Exogenous CXCL12 was revealed to significantly promote the migration and proliferation of HLFs, and potentiate CXCR4 expression. These effects were demonstrated to be inhibited by AMD3100, which is an antagonist of CXCR4. Lung and bronchoalveolar lavage fluid CXCR4 and CXCL12 expression was upregulated by *in vivo* bleomycin administration, which was partially inhibited by pre-treatment with AMD3100. AMD3100 also reduced lung collagen content in the bleomycin model. Inhibiting CXCR4 was indicated to ameliorate the lung compliance and resistance of pulmonary fibrosis. In conclusion, the results of the present study suggested that autocrine CXCR4/CXCL12 axis is an important mechanism underlying the pathogenesis of idiopathic pulmonary fibrosis, and may serve as a potential therapeutic target that can be used in the treatment of pulmonary disease.

Introduction

Idiopathic pulmonary fibrosis (IPF) is a chronic and progressive fibrotic lung disease, with a median patient survival time of 2.5-3.5 years and an increasing worldwide incidence (1). IPF is characterized by tissue remodeling, fibroblast proliferation and extracellular matrix accumulation in the lung parenchyma. The fibrotic response in IPF appears to be driven by sequential alveolar epithelium injury and the subsequent abnormal wound-healing response, which involves multiple cells and factors (1-3).

Chemokine expression is stimulated by infection and inflammation, which serves an important role in the attraction, recruitment and activation of leukocytes and immune cells (4,5). C-X-C Motif Chemokine Ligand 12 (CXCL12) represents the natural ligand for C-X-C motif chemokine receptor 4 (CXCR4) and has been indicated to play a role in the metastasis of CXCR4-expressing cells (6-8). Fibrocytes originate from the bone marrow, and express hematopoietic (CD34+) and mesenchymal markers [collagen I+ (ColI+) and vimentin+] (9). Increasing experimental evidence has demonstrated that CD45+ ColI+ CXCR4+ fibrocytes can migrate to the lungs, following bleomycin injury, in a CXCL12-dependent manner (10-12). Furthermore, the pathophysiological axis of CXCR4/CXCL12 is an important mediator of the activation of fibrocytes to produce excess extracellular matrix components and to further differentiate into contractile myofibroblasts (10-13). Experimental evidence has revealed that the CXCR4/CXCL12 axis is an important mechanism by which fibrocytes participate in the pathophysiological process of lung fibrosis (10-13). However, an additional study demonstrated that CD45+ ColI+ CXCR4+ fibrocytes make a negligible contribution to lung fibrosis (14). Therefore the direct role of this biological axis in mediating pulmonary fibrosis remains to be accurately determined.

Within hypoxic areas of malignant tumors, it has been demonstrated that CXCL12 is secreted by a variety of cells, including tumor cells, stromal cells and tumor-associated fibroblasts (4,5). It has been indicated that CXCL12 activates specific tumor cells via autocrine and paracrine signaling, and enhances their proliferation by upregulating CXCR4 expression (15-17). Furthermore, CXCR4 can facilitate tumor cell adhesion and resistance to apoptosis (17,18). In conclusion, it can be suggested that CXCR4 is associated with the proliferation, cell trafficking and metastasis of cancer cells.

It was hypothesized that the CXCR4/CXCL12 axis is highly active in IPF and contributes to pathogenesis by

Correspondence to: Dr Huaping Dai, Department of Pulmonary and Critical Care Medicine, Center of Respiratory Medicine, China-Japan Friendship Hospital, Capital Medical University, National Clinical Research Center for Respiratory Diseases, 2 Yinghua Dongjie, Hepingli, Beijing 100029, P.R. China
E-mail: daihuaping@ccmu.edu.cn

Key words: autocrine, C-X-C motif chemokine receptor 4/C-X-C motif chemokine 12 axis, pulmonary fibrosis, fibroblasts

directly targeting human lung fibroblasts through autocrine mechanisms. Furthermore, inhibition of CXCR4 may attenuate lung injury and fibrosis pathologically and physiologically. The current study revealed, through both *in vitro* and *in vivo* experiments, that autocrine CXCR4/CXCL12 contributes to lung fibrosis by directly modulating the activities of lung fibroblasts.

Patients and methods

Patient samples. Tissues from 4 IPF patients were collected by surgical lung biopsy between October 2016 and March 2018. Patients were diagnosed through histological evidence of usual interstitial pneumonia. IPF was diagnosed in accordance with the current guidelines of the American Thoracic Society and the European Respiratory Society (1). Control samples from 4 patients who had been diagnosed with primary spontaneous pneumothorax and received thoracoscopy for stapling air leakage, were collected between November 2016 and May 2018. Patient details are shown in Table I.

Primary human lung fibroblast culture and proliferation assay. Human lung fibroblasts (HLFs) were derived from the lung tissues of 3 patients with IPF (patient nos. 2-4, described in Table I). Control lung fibroblasts were derived from histologically normal lung tissue samples of 3 patients (patient nos. 6-8, described in Table I). HLFs were cultured at 37˚C in a 5% CO_2 incubator using the tissue explant adherent method and morphologically observed. Immunofluorescence staining was used to ensure the identification and purity of the primary-cultured HLFs. The culture procedure and cell characterization were conducted as previously described (19).

The proliferation of normal HLFs was evaluated using a MTT assay (Sigma-Aldrich; Merck KGaA). A total of $5x10^3$ lung fibroblasts were seeded into each well of a 96-well plate with DMEM (HyClone; GE Healthcare Life Sciences) containing 2% FBS (HyClone; GE Healthcare Life Sciences), and cultured for 108 h at 37˚C. The medium was then replaced with 200 μl of PBS containing 250 μg/ml MTT every 12 h. Subsequently, the plates were cultured for an additional 4 h at 37˚C. The PBS in the plate was then carefully removed and the trapped MTT crystals were solubilized with 200 μl of DMSO (Sigma-Aldrich; Merck KGaA) at 37˚C. Absorbance was measured 10 min later using a microtiter plate reader (model Infinite M200; Tecan Group Ltd.) at 490 nm. Each experiment was performed in triplicate.

To investigate the effects of CXCL12 on cell proliferation and expression of CXCR4 and colI, normal HLFs were cultured in 96-well plates ($5x10^3$ cells/well) or six-well plates ($1x10^5$ cells/well) in DMEM with 10% FBS at 37˚C. After 24 h of culture, the cells were starved in FBS-free DMEM overnight and then incubated for 72 h with a variety of concentrations of CXCL12 (0, 0.2, 1, 5, 25 and 125 ng/ml; R&D Systems, Inc.) in DMEM with 2% FBS at 37˚C.

The current study was approved by the ethics committee of the China-Japan Friendship Hospital. All included patients signed informed consent for participation in the present study.

Western blot analysis. The fourth passages of fibrotic HLFs (collected from patient nos. 2-4, described in Table I) or normal HLFs (collected from patient nos. 6-8, described in Table I) and the whole lung tissues from 4 IPF patients and 4 control patients (patient nos. 1-8, described in Table I) were used to determine the expression of CXCR4 and ColI, using a RIPA assay buffer (150 mM NaCl; 10 mM NaF; 1.5 mM $MgCl_2$; 10% glycerol; 1% Triton X-100; 4 mM EDTA; 0.1% SDS; 50 mM HEPES; 1% deoxycholate; pH 7.4) containing complete proteinase and phosphatase inhibitor cocktails (Roche Diagnostics). The cytoplasmic extracts were obtained from lysates after centrifugation at 10,000 x g for 10 min at 4˚C. Protein concentrations were assessed using a BCA kit (Pierce; Thermo Fisher Scientific, Inc.). An equal amount of protein (30 μg for HLFs and 100 μg for lung lysates) were subjected to 10% SDS-PAGE gel and transferred onto a PVDF membrane (EMD Millipore) at 4˚C, 200 mA for 2 h. Membranes were subsequently blocked with 5% non-fat dry milk or BSA (Sigma-Aldrich; Merck KGaA) in TBS (10 mM Tris-HCl; pH 7.6; 150 mM NaCl; 0.1% Tween-20) at room temperature for 1 h and then incubated at 4˚C overnight with the indicated primary antibodies supplied by Abcam: Rabbit anti-CXCR4 antibody (1:500; cat. no. ab181020), rabbit anti-collagen I antibody (1:500; cat. no. ab138492) and mouse anti-β-actin monoclonal antibody (1:1,000; cat. no. ab8226). Immunoreactive bands were detected via incubation for 1 h with the appropriate secondary, HRP-labeled antibodies supplied by ProteinTech Group, Inc.: HRP-conjugated Affinipure Goat Anti-Rabbit IgG (1:2,000; cat. no. SA00001-1), HRP-conjugated Affinipure Goat Anti-Mouse IgG (1:2,000; cat. no. SA00001-2), and visualized using an ECL buffer (KPL; Kirkegaard & Perry Laboratories, Inc.) with ChemiDoc XRS (Bio-Rad Laboratories, Inc.). Relative protein levels were calculated by densitometry using Quantity One version 4.6.6 (Bio-Rad Laboratories, Inc.) or Image J version 1.42q (National Institutes of Health). The study of human lung tissues was approved by the ethics committee of the China-Japan Friendship Hospital. All investigated subjects signed an informed consent form consenting to institutional guidelines.

Migration assay. In the transwell migration assay, 24-well culture inserts with porous polycarbonate membrane (8.0 μm pore size; EMD Millipore) were used. A total of $10x10^3$ Normal HLFs were seeded into 60 mm dishes and grew to 80% confluence at 37˚C in a 5% CO_2 incubator. Cells were then serum-starved in DMEM for 24 h and incubated with CXCL12 (final concentration, 5 ng/ml) in the absence or presence of the CXCR4 antagonist AMD3100 (100 ug/ml; Sigma-Aldrich; Merck KGaA) for 1 h at 37 ˚C prior to stimulation. Subsequently, the cells were resuspended and loaded into the upper compartment of the migratory well at a density of $10x10^3$ cells in 100 μl of serum free DMEM. In the lower compartment, 500 μl of DMEM was supplemented with 10% FBS in the absence or presence of CXCL12 (200 ng/ml). After incubation for 24 h at 37˚C, the cells on the lower side of the chambers were fixed with 4% formaldehyde solution for 30 min, stained using crystal violet solution (Sigma-Aldrich: Merck KGaA) for 10 min at room temperature and counted using a light microscope in 6 randomly selected fields (magnification, x100).

Pulmonary fibrosis model building and AMD3100 treatment. Female C57BL/6 mice (age, 6-8 weeks; weight, 18-22 g; n=10 per

Table I. General data of included subjects.

Patient	Age (yr)	Sex (M/F)	Smoker (Y/N)	SCD (year/month)	Diagnosis
1	68	M	N	2016/Oct	IPF
2	64	M	N	2017/Nov	IPF
3	64	M	N	2017/Nov	IPF
4	58	M	N	2018/Mar	IPF
5	52	M	N	2016/Nov	Pneumothorax
6	21	F	N	2018/Feb	Pneumothorax
7	16	M	N	2017/Dec	Pneumothorax
8	30	M	N	2018/May	Pneumothorax

SCD, sample collection date; IPF, idiopathic pulmonary fibrosis.

experimental group) were purchased from the Animal Center of Peking University Health Science Center and maintained under specific pathogen-free conditions at 25±2˚C in a 12 h night/dark cycle. The protocols were approved by the Committee on the Ethics of Animal Experiment of Capital Medical University.

All animals were randomly divided into three groups. A total of 5 mg/kg bleomycin (BLM; Haizheng Pharmaceutical Co., Ltd.) in 50 μl PBS was intratracheally injected, or the equivalent volume of PBS was used as a control, following anesthetization with intraperitoneal injections of pentobarbital sodium (80 mg/kg). Mice in the AMD3100 treatment group received an intraperitoneal injection 200 μg of AMD3100 in 250 μl sterile PBS 1 day prior to bleomycin injection. Mice in the bleomycin group received 250 μl PBS instead of AMD3100. Mice were euthanized using pentobarbital on day 3, 7, 14 and 21 following exposure to bleomycin.

Spirometry. Lung function was measured using a method outlined in a previous study (20). Each animal in the three groups was weighed and anesthetized with an intraperitoneal injection of pentobarbital sodium at a dose of 80 mg/kg on day 21. The tracheal intubation was connected to a computerized small animal ventilator (SCIREQ® flexiVent; SCIREQ Scientific Respiratory Equipment, Inc.; emka Technologies). All mice were mechanically ventilated with 21% O_2 at 150 breaths/min and a tidal volume of 10 ml/kg. After 3 min of mechanical ventilation, rocuronium bromide (0.6 mg/kg) was injected intraperitoneally to paralyze all animals. The volume signal generated using a computer was applied to the airway opening. After a deep inspiration under 30 cm H_2O airway pressure, the quasi-static pressure-volume (P-V) curve was performed *in situ*, and the impedance of the respiratory system was measured under positive end-expiratory pressures of 2 cm H_2O. The parameter K of the P-V curve and relevant data of airway resistance (R) and compliance (C) were obtained using the flexiVent system.

Bronchoalveolar lavage fluid. After testing the lung function, mice were euthanized using pentobarbital overdose and the whole lung was removed via thoracotomy. Bronchoalveolar lavage fluid (BALF) from the whole lung was collected using an 800 μl aliquot of PBS, and this was repeated twice. The collected fluids were centrifuged at 4˚C for 5 min at 160 x g. The supernatants were collected and stored at -80˚C until cytokine analyses. According to the manufacturer's protocol, the concentrations of CXCL12 in HLFs supernatant, and in the mouse BALF and lung homogenates, were determined using human and mouse CXCL12 Quantikine ELISA kits (cat. nos. DSA00 and MCX120; R&D Systems, Inc.).

Collagen assay in lung tissue. The total amount of collagen in mouse lung tissues was determined using the SIRCOL Collagen Assay kit (Biocolor Ltd.) according to the manufacturer's protocol. Extracts derived from left lung lobe homogenates were incubated with Sirius red dye at room temperature for 30 min. Then absorbance at 540 nm was determined using a spectrophotometer (Model, Infinite M200; Tecan Group Ltd.). The amount of collagen is presented in μg per mg of wet tissue.

Histological examination. The excised lungs were perfused with saline and inflated with 1 ml of 4% paraformaldehyde. Lungs were then ligated at the trachea and immersed in 4% paraformaldehyde at 4˚C for 24 h. The fixed lung was embedded in paraffin, cut into 5 μm sections, and stained with hematoxylin and eosin for 5 min or Masson's trichrome for 30 min at room temperature following a standard protocol. For grading lung fibrosis, a numerical fibrotic scale was used (Ashcroft score) (21). All histological specimens were randomly numbered and examined by three pathologists who were blinded to the treatment. The severity of fibrosis in each lung section was assessed as a mean fibrotic score from observation under a light microscopic in 6 randomly selected fields (magnification, x200).

Statistical analysis. Continuous data were presented as the mean ± SEM. Differences between two groups were analyzed using a two-tailed unpaired Student's t-test, while one-way ANOVA with a Bonferroni post-hoc test was used for comparisons of multiple groups. All analyses were performed using SPSS version 13.0 (SPSS, Inc.). $P<0.05$ was considered to indicate a statistically significant difference.

Results

Clinical samples indicate a high expression level of chemokine receptor CXCR4 in IPF lungs. Increasing experimental

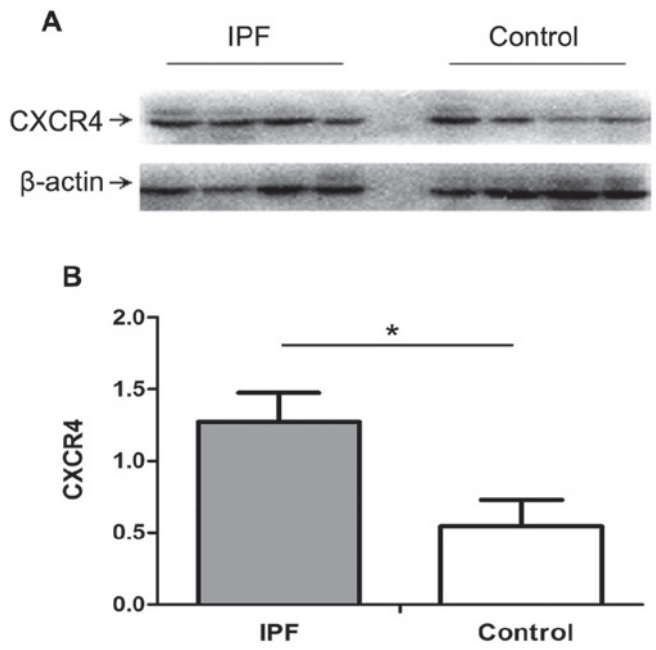

Figure 1. Expression of CXCR4 in lung tissues. The expression of CXCR4 was increased in IPF lung tissues compared with normal lung tissues, as indicatedindicated by (A) western blot analysis and (B) statistical analysis. Values are presented as mean ± SEM. n=4 for each group. *P<0.05 vs. control group. CXCR4, C-X-C Motif Chemokine Receptor 4; IPF, idiopathic pulmonary fibrosis.

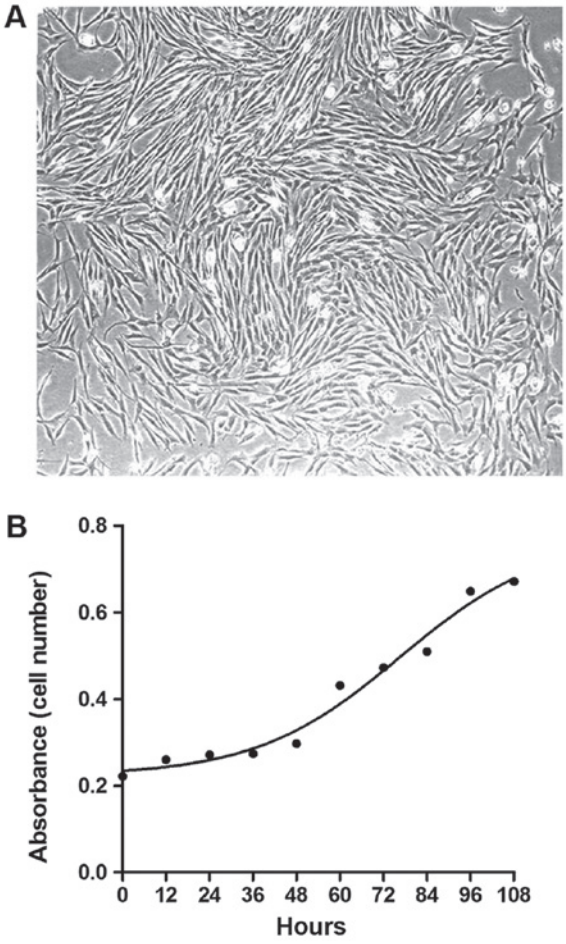

Figure 2. Proliferation of primary human fibroblasts. (A) Primary HLFs displayed typical spindle-shaped morphology (magnification, x40). (B) The growth curve of HLFs indicated a doubling time of ~72 h. HLFs, human lung fibroblasts.

evidence has indicated that CXCR4/CXCL12 is associated with the pathogenesis of lung fibrosis (10-13). Therefore, it was hypothesized that the level of CXCR4 would be significantly increased in lung tissue. To determine this, the current study aimed to examine whether CXCR4 was upregulated in IPF. Proteins extracted from lung tissues of patients with IPF and non-IPF controls were analyzed for CXCR4 expression using western blot analysis. As presented in Fig. 1, compared with normal controls, subjects diagnosed with IPF exhibited higher expression of CXCR4 in lung tissues (P<0.05).

Proliferation of primary human lung fibroblasts. To determine the role of CXCR4/CXCL12 in pulmonary fibrosis, primary human lung fibroblasts were cultured from lung tissues of 3 patients with IPF (fibrotic HLFs) and 3 patients with primary spontaneous pneumothorax (normal HLFs). As presented in Fig. 2A and in previous data (19), primary HLFs had a typical spindle-shaped appearance under a phase-contrast light microscope and were identified by positive staining for vimentin, fibronectin and collagen III, and negative staining for vWF, ProSP-C and α-SMA (19). The growth curve of the fourth normal HLF passages was presented in Fig. 2B, indicating that HLFs grow relatively rapidly, with an approximate doubling time of 72 h. Therefore, this time-point was subsequently used to assess the proliferation effect of CXCL12 on HLFs.

High expression of CXCR4 and collagen and autocrine secretion of CXCL12 by fibrotic HLFs. The cellular sources and targets of CXCR4-CXCL12 remain to be determined. Therefore, the current study examined the positive regulation of the CXCR4/CXCL12 axis in passage 4 HLFs. Whole cell lysates were subjected to western blot analysis. As presented in Fig. 3A-C, CXCR4 and collagen I expression were significantly upregulated in fibrotic HLFs compared with normal HLFs (P<0.05). The supernatant of fibrotic and normal HLFs was collected for ELISA to determine the extracellular level of CXCL12. As presented in Fig. 3D, fibrotic and normal HLFs secreted CXCL12. The secretion level of CXCL12 in fibrotic HLFs was significantly higher compared with normal HLFs (P<0.01). These results indicated that HLFs (especially fibrotic HLFs) are potential cellular sources and targets of CXCL12.

Significant inhibition of HLFs proliferation, and CXCR4 and collagen I protein production following blocking of CXCR4. To determine whether CXCL12 directly induced HLFs proliferation and CXCR4 and collagen I protein production, normal HLFs were exposed to a variety of CXCL12 concentrations (0, 0.2, 1, 5, 25 and 125 ng/ml) for 72 h, and cell growth and protein expression were assessed using an MTT assay and western blot analysis, respectively. As presented in Fig. 4A and B, compared with the control group (medium without CXCL12), HLFs proliferation was induced by CXCL12 in a dose-dependent manner at levels below 5 ng/ml. The maximum growth response was indicated at a dose of 5 ng/ml, and this proliferation reaction was significantly inhibited

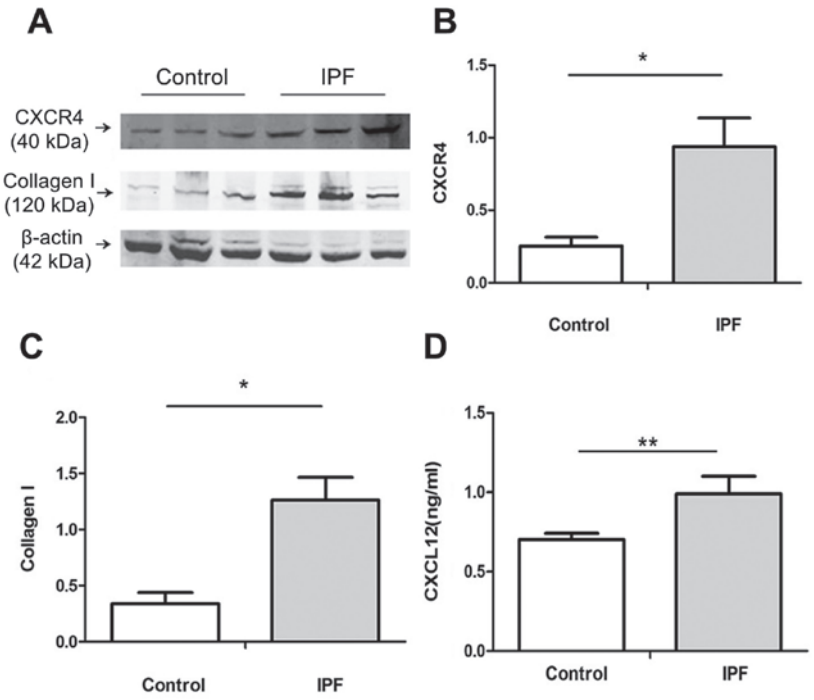

Figure 3. CXCR4 and Collagen I expression were upregulated, and autocrine secretion of CXCL12 was increased in fibrotic HLFs compared with normal HLFs. (A) Western blot analysis indicating the expression of (B) CXCR4 and (C) Collagen I in fibrotic and normal HLFs. (D) Fibrotic and normal HLFs secreted CXCL12, and the secretion level of CXCL12 in fibrotic HLFs was significantly increased compared with normal HLFs, as indicated by ELISA analysis. Values are presented as mean ± SEM. n=3 for each group. *P<0.05 vs. control group; **P<0.01 vs. control group. CXCR4, C-X-C Motif Chemokine Receptor 4; CXCL12, C-X-C Motif Chemokine Ligand 12; HLFs, human lung fibroblasts; IPF, idiopathic pulmonary fibrosis.

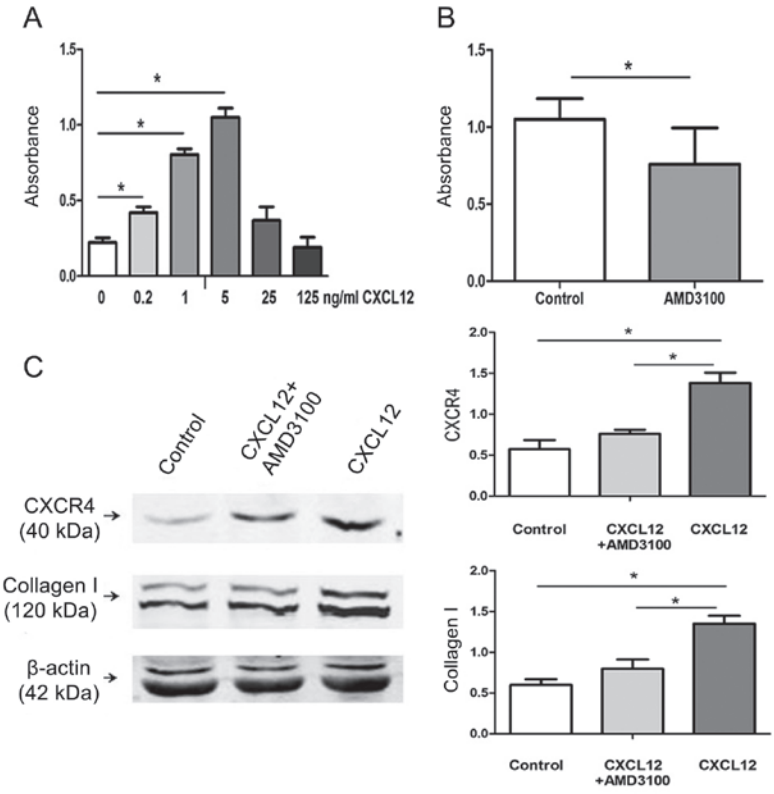

Figure 4. CXCL12 induced HLFs proliferation and CXCR4 and Collagen I protein production. (A) Sub-confluent cultures of HLFs were exposed to a variety of CXCL12 concentrations. HLFs proliferation was induced in a dose-dependent manner below 5 ng/ml. The maximum growth response was observed at the treatment dose of 5 ng/ml. *P<0.05 vs. control group. (B) The CXCL12 induced proliferation of HLFs was significantly inhibited following blockage of CXCR4. *P<0.05 vs. control group. (C) Normal HLFs were either untreated or pretreated for 1 h with the indicated concentrations of AMD3100, followed by CXCL12 treatment (5 ng/ml) for 24 h. Compared with control group (medium, without CXCL12), CXCL12 treatment induced CXCR4 and Collagen I expression, and this effect was reduced by pre-treatment with AMD3100. Values are presented as mean ± SEM. n=3 for each group. *P<0.05. CXCL12, Chemokine Ligand 12; HLFs, human lung fibroblasts; CXCR4, C-X-C Motif Chemokine Receptor 4.

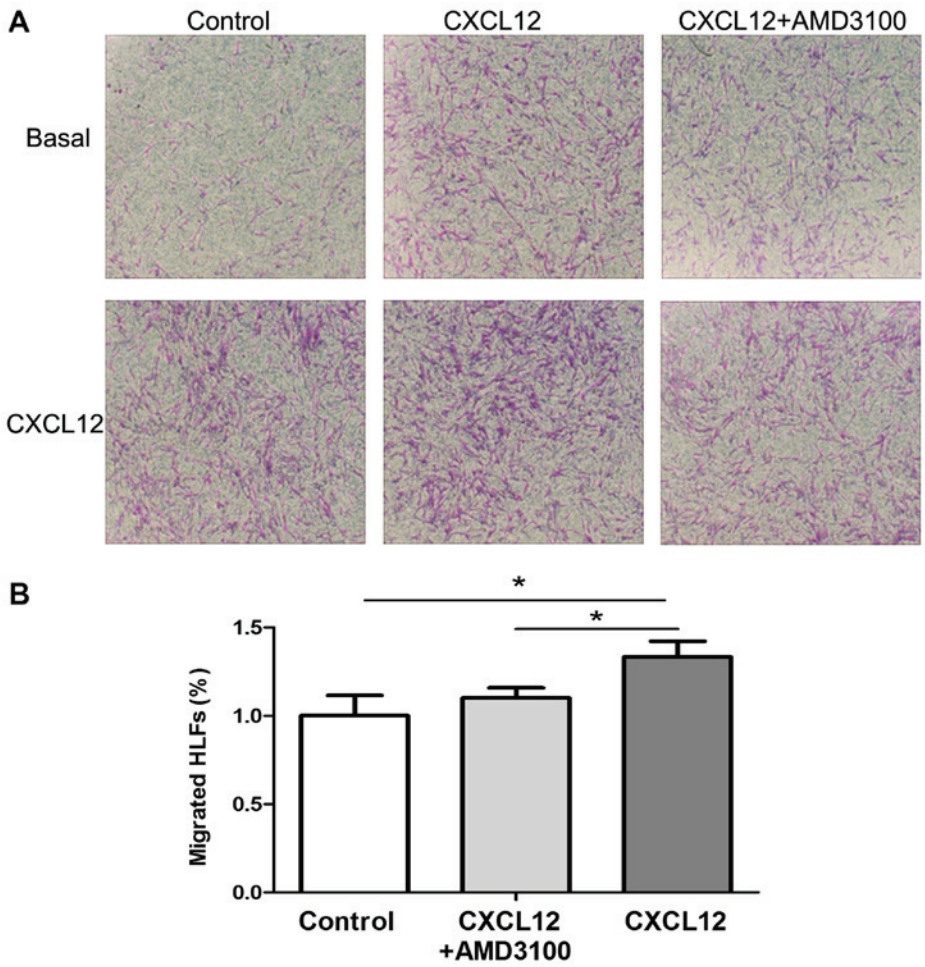

Figure 5. CXCL12 induced HLFs migration. Cells incubated with CXCL12 in the absence or presence of AMD3100 pre-stimulation in serum-free DMEM were added to the upper chamber and medium supplemented with 10% FBS in the absence or presence of CXCL12 were placed in the lower chamber. (A) Photographs of cresyl violet-stained membranes (magnification, x100). (B) Quantitative analysis of numbers of migrated HLFs compared with the control group (with CXCL12 in the lower chamber). CXCL12 incubation significantly increased HLFs migration, which was notably inhibited by AMD3100 pre-stimulation. Values are presented as mean ± SEM. n=3 for each group. *P<0.05. CXCL12, C-X-C Motif Chemokine Ligand 12; HLFs, human lung fibroblasts.

following the use of a CXCR4 receptor antagonist (P<0.05). Subsequently, HLFs were treated with CXCL12 at a concentration of 5 ng/ml in the presence or absence of AMD3100, an antagonist of CXCR4, and their effects on CXCR4 and collagen I expression were determined. Fig. 4C indicated that compared with the control group (medium without CXCL12), CXCL12 treatment significantly induced CXCR4 and collagen I expression, and this effect was reduced by pre-treatment with AMD3100 (P<0.05). These results demonstrated that inhibition of CXCR4 signaling can inhibit HLFs proliferation and CXCR4 and collagen I protein production.

CXCL12 is required for HLFs migration. The development of lung fibrosis has been suggested to be associated with fibroblast recruitment into the sites of lung injury (1-3,9). A previous study revealed that CXCL12 can be secreted by HLFs (22). To determine the effect of CXCL12 on HLFs migration, an *in vitro* chemotaxis assay was performed. As indicated in Fig. 5, CXCL12 incubation significantly increased HLF migration (P<0.05), which was significantly inhibited by AMD3100 pre-stimulation (P<0.05). The results demonstrated that the CXCR4/CXCL12 chemokine axis promoted the migration of HLFs.

A CXCR4 antagonist attenuates pulmonary fibrosis and decreases the protein expression of CXCL12 and CXCR4. In accordance with previous studies (10-13), the current study indicated that AMD3100 treatment significantly attenuated the BLM-induced pulmonary inflammation and fibrosis, as determined by histological examination and fibrosis score on day 21 compared with the bleomycin group (Fig. 6). To evaluate the therapeutic value of AMD3100 *in vivo*, the effect of AMD3100 treatment on lung collagen content following BLM challenge was also assessed (Fig. 7A). The collagen deposition in response to BLM was decreased in the BLM + AMD3100 group, which was more obvious on day 21, compared with BLM group (P<0.05). The protein levels of CXCL12 and CXCR4 were also determined. As presented in Fig. 7B, the concentrations of CXCL12 protein in BALF and lung homogenates from BLM treated mice increased from day 3, peaked on day 7, and then decreased gradually to the levels of control group on day 21. AMD3100 pre-treatment decreased the levels of CXCL12 on day 3 and day 7 (P<0.01). BLM upregulated the expression of CXCR4 in lung tissue, which reached a plateau on day 7. AMD3100 treatment significantly reduced the levels of CXCR4 after day 14 (P<0.01 vs. bleomycin group; Fig. 7C).

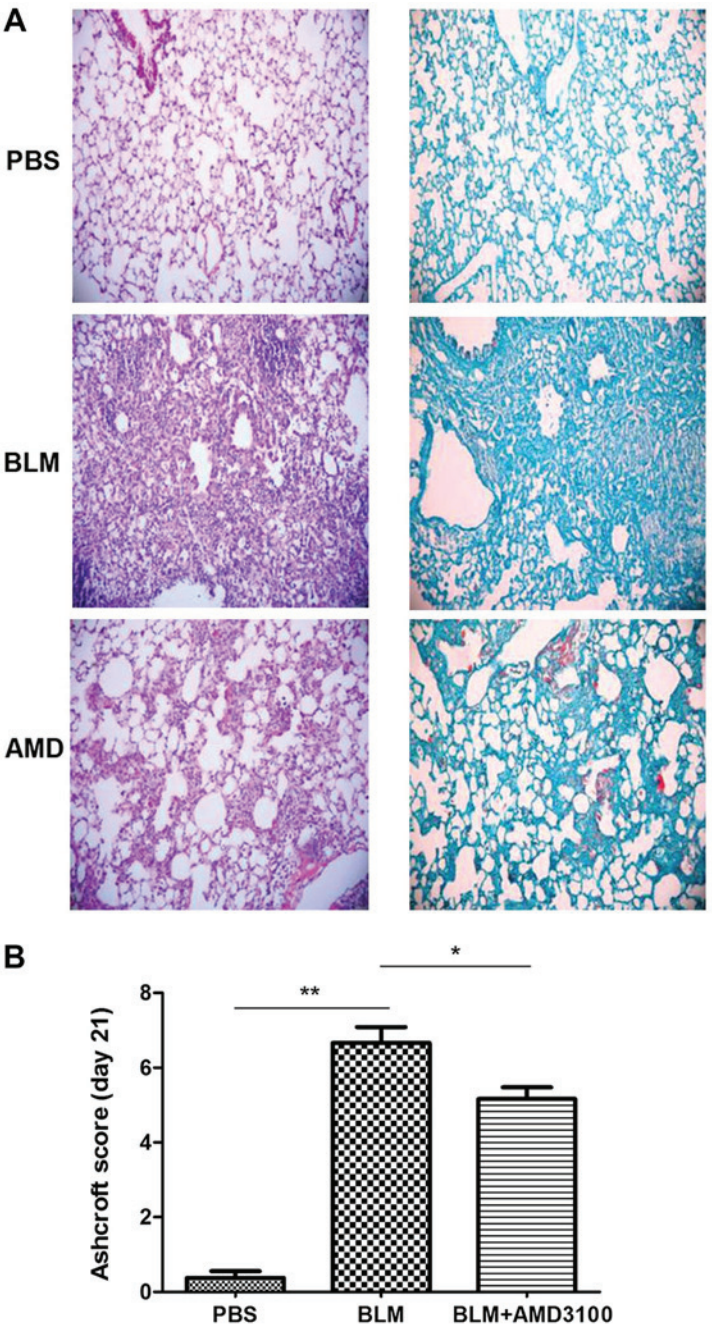

Figure 6. Treatment of AMD3100 attenuated bleomycin-induced pulmonary fibrosis in mice. (A) Representative images of Hematoxylin-Eosin and Masson's trichrome staining of lung sections, respectively (magnification, x200). Bleomycin induced significant pulmonary inflammation and fibrosis, which peaked on day 21. This histological change was markedly reduced by AMD3100 treatment. (B) Pulmonary fibrosis on day 21 was scored by Ashcroft method. Data are expressed as mean ± SEM. *P<0.05, **P<0.01. n=10 for each group.

Inhibition of CXCR4 ameliorates lung function in pulmonary fibrosis. Lung function tests were performed in three groups of mice on day 21 following exposure to PBS, BLM and AMD3100. The P-V curve obtained is a typical curve of the first inflation and deflation under degassing conditions and the second complete curve to 30 cm H_2O. As presented by the P-V curve (Fig. 8A), the maximal lung volume was decreased after BLM challenge, compared with the control group. However, AMD3100 treatment appeared to reduce this disparity. The parameter K, which is an indirect representation of lung elasticity, indicated the curvature of the upper portion of the deflation P-V curve. This parameter of BLM group was significantly lower than that of the PBS group, and treatment with AMD3100 increased the parameter K (Fig. 8B; P<0.05). A similar variation of parameter K patterns were observed in terms of compliance. The Quasi-static compliance indicated the static elastic recoil pressure of the lungs at a given lung volume. The decrease in compliance was significantly greater in BLM group compared with the AMD3100 group (Fig. 8C; P<0.05). The resistance of BLM group was increased, which was significantly inhibited by AMD3100 pretreatment (Fig. 8D; P<0.05). The aforementioned findings implied that blockage of CXCR4 ameliorated the lung compliance and resistance in pulmonary fibrosis.

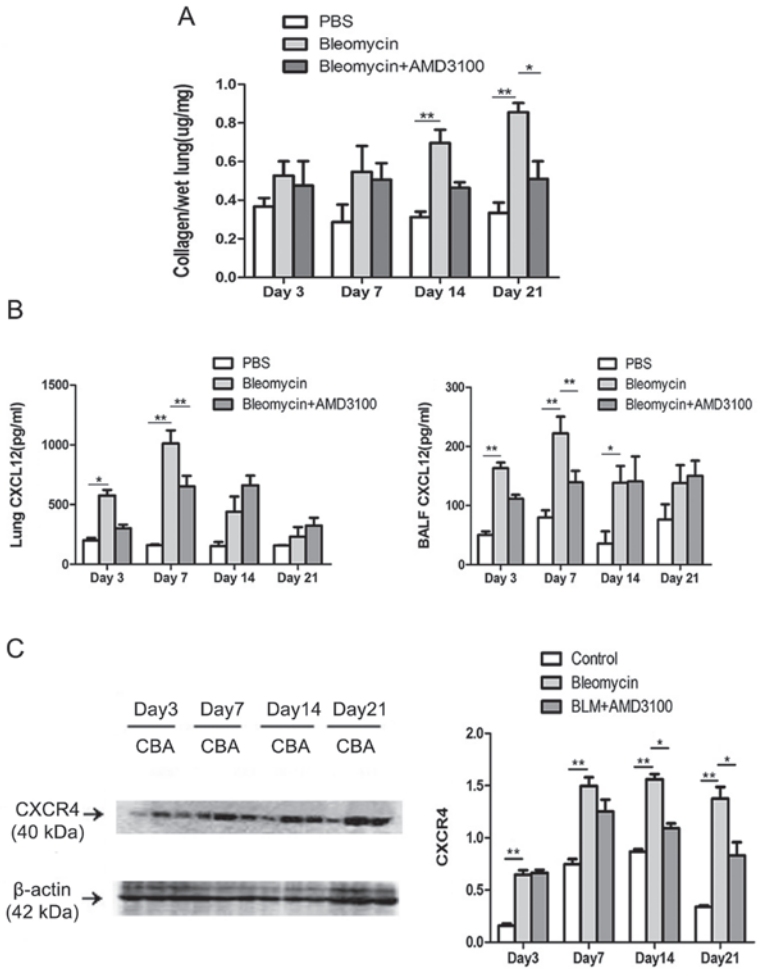

Figure 7. Treatment of AMD3100 attenuated bleomycin-induced pulmonary fibrosis in mice. (A) SIRCOL assay for the total collagen content in lungs. The bleomycin-induced pulmonary fibrosis progressed and resulted in severe changes on days 14 and 21. This histological change was markedly reduced by AMD3100 treatment. (B) The protein level of CXCL12 in lung homogenates and the BALF of mice in 3 groups were determined using an ELISA. Concentrations of CXCL12 peaked on day 7 and then decreased, and AMD3100 treatment decreased the levels of CXCL12. The reduction of CXCL12 induced by AMD3100 in lung tissues on day 7 was statistically significant compared with the bleomycin group ($P<0.01$) and exhibited no effect after day 7. (C) Western blot analysis indicated that CXCR4 was increased from 3 days to 21 days after bleomycin injury. AMD3100 treatment decreased CXCR4 protein level. C, control; B, bleomycin; A, bleomycin + AMD3100. Data are expressed as mean ± SEM. $^{*}P<0.05$, $^{**}P<0.01$; n=5-7 for each group.

Discussion

IPF is a progressive fibrotic lung disease with a poor prognosis following the initial diagnosis (1). However, the pathologic profiles for pulmonary fibrosis are poorly understood (1). Fibroblasts are considered to be the master switch of IPF by synthesizing ECM in fibroblastic foci (the histopathological hallmarks of IPF) (1-3). In the current study, the effect of the CXCR4/CXCL12 axis on the proliferation and ECM metabolism of primary HLFs was assessed. It was indicated that CXCL12 aggravated proliferation and migration of HLFs, and increased collagen release by direct autocrine stimulation via CXCR4, which could be attenuated by AMD3100 pretreatment.

Chemokines and receptors are recognized universally to be crucial in the process of leukocyte recruitment, especially at sites of tissue injury, cell damage and infection (23-25). CXCR4 is a chemokine receptor for the ligand of CXCL12. CXCR4/CXCL12 axis is functional in a number of organs including the lung, heart, kidney and liver. The present study identified high expression of CXCR4 in lung tissues with pulmonary fibrosis and indicated that high expression may contribute to lung injury and fibrosis, and subsequent research confirms this point.

Multiple cell types can express CXCR4/CXCL12 in lung tissues (especially in fibrotic lungs), including fibroblasts, epithelial cells, vascular endothelial cells and some inflammatory cells (26-29). As previously reported, a major population of CXCR4+ cells was localized close to the fibroblastic foci in lung tissue sections from patients with IPF (28,29). CXCL12 was indicated to be upregulated in reactive hyperplastic alveolar epithelial cells often overlying fibroblastic foci, and staining for this was also observed in endothelial cells and some alveolar macrophages, except for the normal areas of the IPF lungs (28), supporting the notion that these cells serve a role in the pathogenesis of IPF. The results of the current study demonstrated that primary human lung fibroblasts in adult pulmonary fibrosis can express and secrete CXCL12, and can respond to the extraneous CXCL12 by binding to their own receptor, CXCR4. This indicated that the autocrine CXCR4/CXCL12 axis resides in lung fibroblasts and contributed to lung fibrosis by directly activating lung fibroblasts.

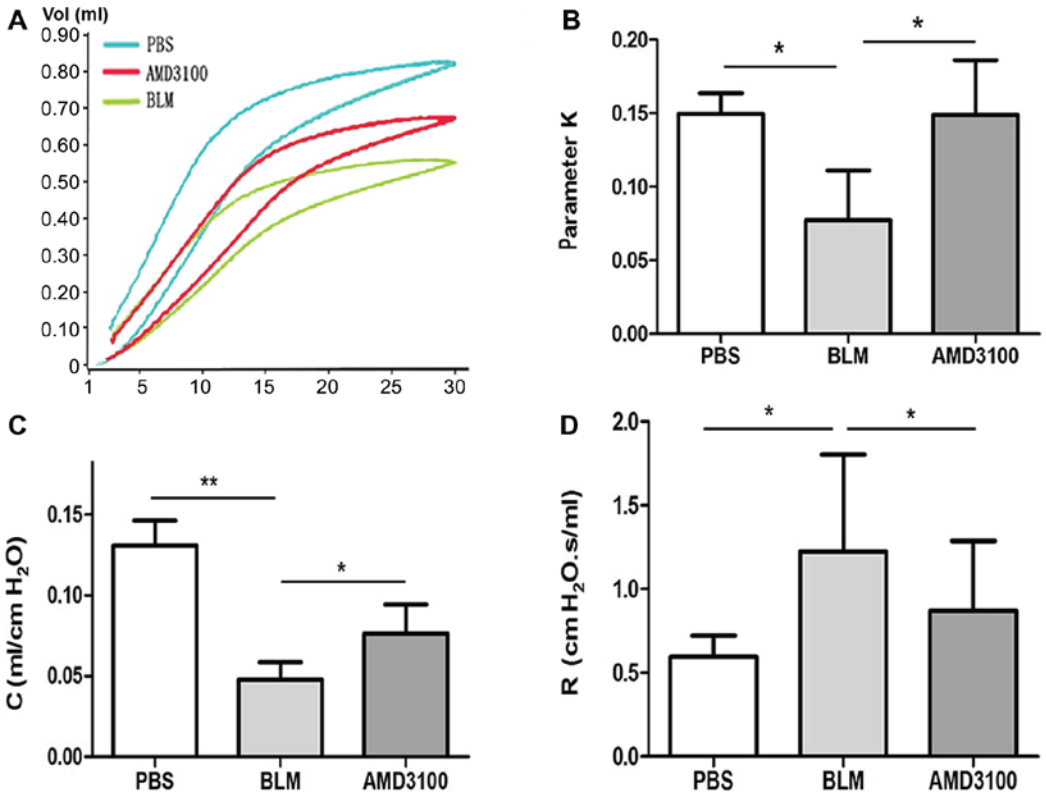

Figure 8. Pulmonary dysfunction was compared between the three groups. (A) Quasi-static P-V curves were measured at PEEP of 30 cm H_2O. The maximal lung volume of BLM group was significantly decreased, compared with the PBS group, and AMD3100 pretreatment alleviated the decrease in lung volume. The decrease in (B) parameter K and (C) Compliance was significantly greater in the BLM group compared with the AMD3100 group. (D) The resistance of BLM group was increased, which was notably inhibited by AMD3100 pre-treatment. Data are expressed as the mean ± SEM. *P<0.05, **P<0.01; n=5 for each group. PEEP, positive end-expiratory pressures; BLM, bleomycin; C, compliance; R, resistance.

A number of studies have demonstrated that CXCR4/CXCL12 participates in cancer development (6,8,15-18). CXCR4 is the only chemokine receptor expressed by the majority of cancer cells, and its ligand CXCL12 can be secreted by tumor cells and stromal cells, including tumor-associated fibroblasts (24,25). The underlying mechanism of this is yet to be determined. Increasing evidence has demonstrated that binding CXCL12 to CXCR4 stimulates the proliferation of a variety of tumor cell lines and their migration and adhesion to ECM components by the activation of downstream signal transduction pathways. For example, Lin CH *et al* (30) demonstrated that CXCL12, acting through CXCR4 and activating the Rac/ERK and JNK signaling pathways, could induce the expression of connective tissue growth factor, which is a profibrotic protein, in human lung fibroblasts, and potentiate their transdifferentiation into myofibroblasts. Wang X *et al* (16) demonstrated that the autocrine CXCL12/CXCR4 axis can mediate the metastatic property of esophageal cancer stem cells depending on ERK1/2 signaling pathway. Tian Y *et al* (31) indicated that CXCL12 induced the migration of oligodendrocyte precursor cells via the CXCR4 dependent MEK/ERK and PI3K/AKT pathways. The increased expression of FOXM1 has been demonstrated to induce apoptosis resistance in fibroblasts and contribute to lung fibrosis (32). A previous study has also revealed that PI3Kα signaling via PDK1/AKT could mediate FGF2-induced FOXM1 upregulation in lung fibroblasts (32). Furthermore, FOXM1 signaling mediated vascular remodeling and pulmonary hypertension, as previously reported (27). Collectively, these studies indicated that PI3K/AKT and MEK/ERK pathways and FOXM1 may serve as potential post-receptor signaling pathways that mediate the profibrotic effect of CXCL12 in lung fibroblasts. However, this still remains to determined in the future.

Previous studies on CXCR4/CXCL12 have focused on CD45 + Col I + CXCR4 + fibrocytes, which are one of the origins of the fibroblasts/myofibroblasts (10-13,28,29). A previous study suggested that fibrocytes are not a necessary source of collagen during pulmonary fibrosis, and indicated that fibrocyte may make other contributions to collagen accumulation, including activating fibroblasts to secrete CXCL12 and aggregating other fibrotic effector cells and factors to release CXCL12 to act on fibroblasts (14). Recent studies using lineage tracing to explore the origins of myofibroblasts in models of lung fibrosis have concluded that resident lung fibroblasts are their major source (33,34). Lung biopsies from patients with IPF indicated an increase in the number of fibroblasts, which is likely due to increased proliferation (3). The current study demonstrated that CXCL12 potentiated proliferation in primary HLFs. The strategical blocking of the CXCR4/CXCL12 axis may be an effective approach to inhibit the cellular activities of HLFs.

In line with prior trails (12), the results of the present study demonstrated that the concentration of CXCL12 was increased late in BALF and lung homogenates after bleomycin

instillation. This increase in CXCL12 was accompanied by an increase in CXCR4 expression in the lungs with a peak at the third week following injury. Currently, it is believed that inflammation is associated with the formation of pulmonary fibrosis, and a variety of inflammatory cells, including neutrophils and lymphocytes, release a variety of inflammatory factors, including CXCL12. In this cascade reaction, the increased concentration of CXCL12 leads to the expression of its receptor CXCR4, which further promotes the proliferation of fibroblasts and further aggravates pulmonary fibrosis (9). Treatment of mice with AMD3100, the CXCR4 antagonist, decreased the production of CXCR4/CXCL12 and attenuated bleomycin induced lung fibrosis, despite incomplete inhibition.

It has been well established that pulmonary fibrosis is a restrictive ventilatory dysfunction due to reduced lung volume and decreased compliance (2). With the alleviation of pulmonary fibrosis, pulmonary function will be improved. Furthermore, the current study measured the lung function of fibrotic mice. It was demonstrated that blocking CXCR4 could not only alleviate pulmonary fibrosis pathologically, but also physiologically. The whole lung resistance of mice decreased significantly, and the pulmonary elasticity also improved significantly. This is the first study exploring the autocrine mechanism of CXCR4/CXCL12 axis in the pathogenesis of pulmonary fibrosis; however, the current study has limitations due to the small number of studied subjects. Future research using a large cohort and long-term follow-up is required to prove the autocrine mechanism of CXCR4/CXCL12 axis in the pathogenesis of pulmonary fibrosis.

In conclusion, the current study demonstrated that fibroblasts are the cellular sources and targets of CXCL12, due to the autocrine secretion of excessive amount of CXCL12 and over-expression of the corresponding receptor CXCR4. The current study indicated the important role of the CXCR4/CXCL12 chemokine axis in the proliferation, migration and collagen production of HLFs *in vivo* and *in vitro*. Blocking this axis could partially attenuate pulmonary fibrosis pathologically and physiologically. These findings demonstrated that the CXCR4/CXCL12 axis could be a potential therapeutic target that may be used in the treatment of pulmonary disease.

Acknowledgements

Not applicable.

Funding

The present study was supported by grants from the National Natural Science Foundation of China (grant nos. 81430001 and 81470258).

Availability of data and materials

The datasets used and/or analyzed during the current study are available from the corresponding author on reasonable request.

Authors' contributions

FL designed and performed the experiments, analyzed the data, drafted and revised the manuscript. XX, JG and XW participated in the experiments and analysis of the data. HD contributed to the conception and design of the present study, the analysis and interpretation of the data, revision of the article and final approval of the version to be published. All authors have read and approved this final manuscript.

Ethics approval and consent to participate

Studies involving human tissues were approved by the Ethics Committee of The China-Japan Friendship Hospital (approval no. 2014-KE-71) and written informed consent was obtained from all investigated subjects. Studies involving animals were approved by the Committee on the Ethics of Animal Experiment of Capital Medical University (approval no. 2014-KE-38).

Patient consent for publication

Not applicable.

Competing interests

The authors declare that they have no competing interests.

References

1. Raghu G, Remy-Jardin M, Myers JL, Richeldi L, Ryerson CJ, Lederer DJ, Behr J, Cottin V, Danoff SK, Morell F, *et al*: Diagnosis of idiopathic pulmonary fibrosis. An official ATS/ERS/JRS/ALAT clinical practice guideline. Am J Respir Crit Care Med 198: e44-e68, 2018.
2. Richeldi L, Collard HR and Jones MG: Idiopathic pulmonary fibrosis. Lancet 389: 1941-1952, 2017.
3. Wolters PJ, Collard HR and Jones KD: Pathogenesis of idiopathic pulmonary fibrosis. Annu Rev Pathol 9: 157-179, 2014.
4. Legler DF and Thelen M: Chemokines: Chemistry, biochemistry and biological function. Chimia (Aarau) 70: 856-859, 2016.
5. Liekens S, Schols D and Hatse S: CXCL12-CXCR4 axis in angiogenesis, metastasis and stem cell mobilization. Curr Pharm Des 16: 3903-3920, 2010.
6. Li J, Li T, Li S, Xie L, Yang YL, Lin Q, Kadoch O, Li H, Hou S and Xu Z: Experimental study of the inhibition effect of CXCL12/CXCR4 in malignant pleural mesothelioma. J Investig Med 67: 338-345, 2019.
7. Miller RJ, Banisadr G and Bhattacharyya BJ: CXCR4 signaling in the regulation of stem cell migration and development. J Neuroimmunol 198: 31-38, 2008.
8. He W, Yang T, Gong XH, Qin RZ, Zhang XD and Liu WD: Targeting CXC motif chemokine receptor 4 inhibits the proliferation, migration and angiogenesis of lung cancer cells. Oncol Lett 16: 3976-3982, 2018.
9. Bagnato G and Harari S: Cellular interactions in the pathogenesis of interstitial lung diseases. Eur Respir Rev 24: 102-114, 2015.
10. Phillips RJ, Burdick MD, Hong K, Lutz MA, Murray LA, Xue YY, Belperio JA, Keane MP and Strieter RM: Circulating fibrocytes traffic to the lungs in response to CXCL12 and mediate fibrosis. J Clin Invest 114: 438-446, 2004.
11. Mehrad B, Burdick MD and Strieter RM: Fibrocyte CXCR4 regulation as a therapeutic target in pulmonary fibrosis. Int J Biochem Cell Biol 41: 1708-1718, 2009.
12. Xu J, Mora A, Shim H, Stecenko A, Brigham KL and Rojas M: Role of the SDF-1/CXCR4 axis in the pathogenesis of lung injury and fibrosis. Am J Respir Cell Mol Biol 37: 291-299, 2007.
13. Makino H, Aono Y, Azuma M, Kishi M, Yokota Y, Kinoshita K, Takezaki A, Kishi J, Kawano H, Ogawa H, *et al*: Antifibrotic effects of CXCR4 antagonist in bleomycin-induced pulmonary fibrosis in mice. J Med Invest 60: 127-137, 2013.
14. Kleaveland KR, Velikoff M, Yang J, Agarwal M, Rippe RA, Moore BB and Kim KK: Fibrocytes are not an essential source of type I collagen during lung fibrosis. J Immunol 193: 5229-5239, 2014.

15. Barbero S, Bonavia R, Bajetto A, Porcile C, Pirani P, Ravetti JL, Zona GL, Spaziante R, Florio T and Schettini G: Stromal cell-derived factor 1alpha stimulates human glioblastoma cell growth through the activation of both extracellular signal-regulated kinases 1/2 and Akt. Cancer Res 63: 1969-1974, 2003.
16. Wang X, Cao Y, Zhang S, Chen Z, Fan L, Shen X, Zhou S and Chen D: Stem cell autocrine CXCL12/CXCR4 stimulates invasion and metastasis of esophageal cancer. Oncotarget 8: 36149-36160, 2017.
17. Guo S, Xiao D, Liu H, Zheng X, Liu L and Liu S: Interfering with CXCR4 expression inhibits proliferation, adhesion and migration of breast cancer MDA-MB-231 cells. Oncol Lett 8: 1557-1562, 2014.
18. Abraham M, Klein S, Bulvik B, Wald H, Weiss ID, Olam D, Weiss L, Beider K, Eizenberg O, Wald O, *et al*: The CXCR4 inhibitor BL-8040 induces the apoptosis of AML blasts by downregulating ERK, BCL-2, MCL-1 and cyclin-D1 via altered miR-15a/16-1 expression. Leukemia 31: 2336-2346, 2017.
19. Xu X, Wan X, Geng J, Li F, Wang C and Dai H: Kinase inhibitors fail to induce mesenchymal-epithelial transition in fibroblasts from fibrotic lung tissue. Int J Mol Med 32: 430-438, 2013.
20. Huang J, Li Z, Yao X, Li Y, Reng X, Li J, Wang W, Gao J, Wang C, Tankersley CG and Huang K: Altered Th1/Th2 commitment contributes to lung senescence in CXCR3-deficient mice. Exp Gerontol 48: 717-726, 2013.
21. Ashcroft T, Simpson JM and Timbrell V: Simple method of estimating severity of pulmonary fibrosis on a numerical scale. J Clin Pathol 41: 467-470, 1988.
22. Shimizu Y, Dobashi K, Endou K, Ono A, Yanagitani N, Utsugi M, Sano T, Ishizuka T, Shimizu K, Tanaka S and Mori M: Decreased interstitial FOXP3(+) lymphocytes in usual interstitial pneumonia with discrepancy of CXCL12/CXCR4 axis. Int J Immunopathol Pharmacol 23: 449-461, 2010.
23. Buck AK, Stolzenburg A, Hänscheid H, Schirbel A, Lückerath K, Schottelius M, Wester HJ and Lapa C: Chemokine receptor-directed imaging and therapy. Methods 130: 63-71, 2017.
24. Balkwill F: Chemokine biology in cancer. Semin Immunol 15: 49-55, 2003.
25. Balkwill F: The significance of cancer cell expression of the chemokine receptor CXCR4. Semin Cancer Biol 14: 171-179, 2004.
26. Dai Z, Li M, Wharton J, Zhu MM and Zhao YY: Prolyl-4 Hydroxylase 2 (PHD2) deficiency in endothelial cells and hematopoietic cells induces obliterative vascular remodeling and severe pulmonary arterial hypertension in mice and humans through hypoxia-inducible factor-2α. Circulation 133: 2447-2458, 2016.
27. Dai Z, Zhu MM, Peng Y, Jin H, Machireddy N, Qian Z, Zhang X and Zhao YY: Endothelial and smooth muscle cell interaction via FoxM1 signaling mediates vascular remodeling and pulmonary hypertension. Am J Respir Crit Care Med 198: 788-802, 2018.
28. Andersson-Sjöland A, de Alba CG, Nihlberg K, Becerril C, Ramírez R, Pardo A, Westergren-Thorsson G and Selman M: Fibrocytes are a potential source of lung fibroblasts in idiopathic pulmonary fibrosis. Int J Biochem Cell Biol 40: 2129-2140, 2008.
29. Mehrad B, Burdick MD, Zisman DA, Keane MP, Belperio JA and Strieter RM: Circulating peripheral blood fibrocytes in human fibrotic interstitial lung disease. Biochem Biophys Res Commun 353: 104-108, 2007.
30. Lin CH, Shih CH, Tseng CC, Yu CC, Tsai YJ, Bien MY and Chen BC: CXCL12 induces connective tissue growth factor expression in human lung fibroblasts through the Rac1/ERK, JNK, and AP-1 pathways. PLoS One 9: e104746, 2014.
31. Tian Y, Yin H, Deng X, Tang B, Ren X and Jiang T: CXCL12 induces migration of oligodendrocyte precursor cells through the CXCR4-activated MEK/ERK and PI3K/AKT pathways. Mol Med Rep 18: 4374-4380, 2018.
32. Penke LR, Speth JM, Dommeti VL, White ES, Bergin IL and Peters-Golden M: FOXM1 is a critical driver of lung fibroblast activation and fibrogenesis. J Clin Invest 128: 2389-2405, 2018.
33. Rock JR, Barkauskas CE, Cronce MJ, Xue Y, Harris JR, Liang J, Noble PW and Hogan BL: Multiple stromal populations contribute to pulmonary fibrosiswithout evidence for epithelial to mesenchymal transition. Proc Natl Acad Sci USA 108: E1475-E1483, 2011.
34. Xie T, Liang J, Liu N, Huan C, Zhang Y, Liu W, Kumar M, Xiao R, D'Armiento J, Metzger D, *et al*: Transcription factor TBX4 regulates myofibroblast accumulation and lung fibrosis. J Clin Invest 126: 3063-3079, 2016.